Neutron production in neutron-induced reactions at 96 MeV on iron and lead

F.-R. Lecolley[1)], I.C. Sagrado García[1,2)],J.-F. Lecolley[1)], G. Ban[1)], J.-M. Fontbonne[1)], G. Iltis[1)], J.-L. Lecouey[1)], T. Lefort[1)], N. Marie[1)], J.-C. Steckmeyer[1)], Ch. Le Brun[3)], J. Blomgren[4)], C. Johansson[4)], J. Klug[4)], A. Orhn[4)], P. Mermod[4)], N. Olsson[4)], S. Pomp[4)], M. Osterlund[4)], U. Tippawan[4,5)], A.V. Prokofiev[6)], P. Nadel-Turonski[7)], M. Fallot[8)], Y. Foucher[8)], A. Guertin[8)], F. Haddad[8)], M. Vatre[8)]

1) LPC, ENSICAEN, UCBN and CNRS/IN2P3, Caen, France
2) DSM/DAPNIA, CEA-Saclay, France
3) LPSC, Grenoble, France
4) Department of Neutron Research, Uppsala University, Sweden
5) Fast Neutron Research Facility, Chiang Mai University, Thailand
6) The Svedberg Laboratory, Uppsala University, Sweden
7) George Washington University, Washington DC, USA
8) SUBATECH Nantes, France
fr.lecolley@lpccaen.in2p3.fr

Abstract: Double differential cross sections for neutron production were measured in 96 MeV neutron induced reactions at The Svedberg Laboratory (TSL) in Uppsala (Sweden). Measurements for iron and lead targets were performed using two independent set-ups: DECOI-DEMON, a time-of-flight telescope dedicated to the detection of emitted neutrons with energies between few MeV and 50 MeV, and CLODIA-SCANDAL, a device used to measure emitted neutrons with energies above 40 MeV. Double differential cross sections were measured for an angular range between 15 and 100 degrees and with low-energy threshold (1-2 MeV). Elastic cross sections, angular and energy distributions and total inelastic cross sections have been obtained from measured double differential cross sections. After a brief presentation of setups, data reduction and normalization procedure are discussed. The results are then compared with calculations performed with several models and transport codes (MCNPX, GEANT, TALYS and PHITS) and with other experimental data (EXFOR data base).

Introduction

Future Accelerator-Driven Systems (ADS) will coupe a high-energy intense proton beam (1 GeV & a few mA) with a spallation target and a sub-critical reactor core. Protons impinging on the ADS target will yield a large amount of spallation products, mainly neutrons, protons and light charged particles, with energies ranging in the MeV to the GeV region. Below 20 MeV the nuclear data libraries are nearly complete [1]. Above 200 MeV the cross section predictions by Intra Nuclear Cascade (INC) models are in good agreement with the experimental data [2,3,4]. For energies from 20 to 200 MeV there are few high-quality data, most of them for (n,Xlcp) and (p,Xn) obtained in the frame of the HINDAS collaboration [1]. Particularly for (n,Xn) inelastic measurements there is only one experimental measurement [5]. Within this context, the aim of this work included in the European collaboration EUROTRANS-NUDATRA [6] was to measure (n,Xn) double differential cross sections (DDCS). Measurements using lead and iron targets were carried out at The Svedberg Laboratory (TSL), Uppsala (Sweden), where a quasi-monoenergetic neutron beam at 96 MeV is available [7,8]. They were accomplished using two independent set-ups: DECOI-DEMON and CLODIA-SCANDAL which are briefly described in the following section. Then experimental results are presented and compared with several calculations using the main available transport codes. Finally we have used the few existing data to perform a qualitative study of the dependence of (n,Xn) cross sections on the target mass. The last section of this paper will summarize the mains results and conclusions obtained from this work.

Experimental setup

In order to obtain complete distributions, the measurements were carried out using two independent devices. Both devices as well as a detailed description of experimental techniques have been presented in reference [9, 10]
To measure the low-energy part of the neutron spectrum (1 – 50 MeV), a time-of-flight telescope labelled DECOI-DEMON was developed. DECOI is a neutron-to-proton converter made of a plastic scintillator. DEMON is a neutron detector made of a cylindrical scintillator. Incoming neutron, weakly deflected in DECOI, is detected and identified using a DEMON. The neutron energy is determined using the well-known time-of-flight technique.
To measure the high-energy part of the neutron spectrum (40 – 100 MeV) a new set-up labelled CLODIA-SCANDAL was developed. CLODIA consists of seven neutron-to-proton converters and eight multi drift chambers to measure the recoil proton trajectories and determine in which converter the neutron interaction took place. In addition, one SCANDAL arm was used to measure the energy of recoil proton. Neutron energy is deduced from the angle of the well-known backward elastic neutron-proton scattering and from the energy of the recoiling proton.

Experimental results

Figure 1 shows the complete double differential distributions for lead and iron targets for an angular range from 15 to 100 degrees and with an energy threshold of 1 – 2 MeV. Distributions below 50 MeV were obtained using the DECOI-DEMON data, above 40 MeV from measurements involving CLODIA-SCANDAL set-up. In the overlap region of the energy spectra, from 40 to 50 MeV, the two set of measurement are in agreement within 10%. This value corresponds to systematic errors (see [9,10] for details).

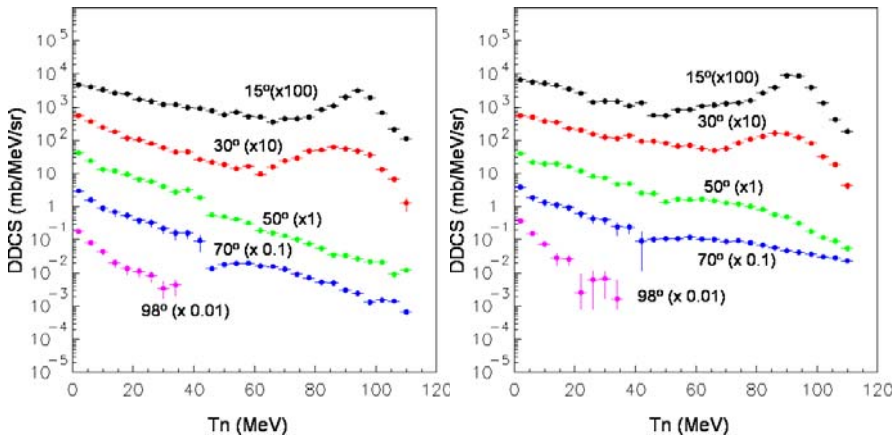

Figure 1. *(n,Xn) measured double differential cross section at 96 MeV for iron (left) and lead (right) in the angular range between 15 and 98 degrees.*

Double differential spectra are characterized by three components:
- a peak at the beam energy. This peak, only present in distributions measured at small angles, is characteristic to direct reactions between incident neutron and a neutron from the target. As expected, this elastic contribution decrease strongly with the emission angle, being more important at 15 degrees than at 30 degrees.
- a peak at low energy (1 – 15 MeV) characteristic for the evaporation process which is the dominant process at backward angles.
- in between these regions one can identify the pre-equilibrium which is a consequence of intra nuclear cascade process. This component also shows a strong dependence on the angle.

For small angles (below 30 degrees) elastic cross section can be calculated from double differential cross sections integrating over the elastic peak. On the other hand the DECOI-DEMON device allows the elastic cross section measurements at all angles [9,10]. The obtained results for lead and iron are compared with the existing experimental data [11,12,13] and with the theoretical calculations based on the optical model [14] (figure 2). Our results for both targets are in good agreement with previous experimental measurements as well as with

the optical model calculations. This allows the validation of the normalization procedure used to extract the double differential cross sections.

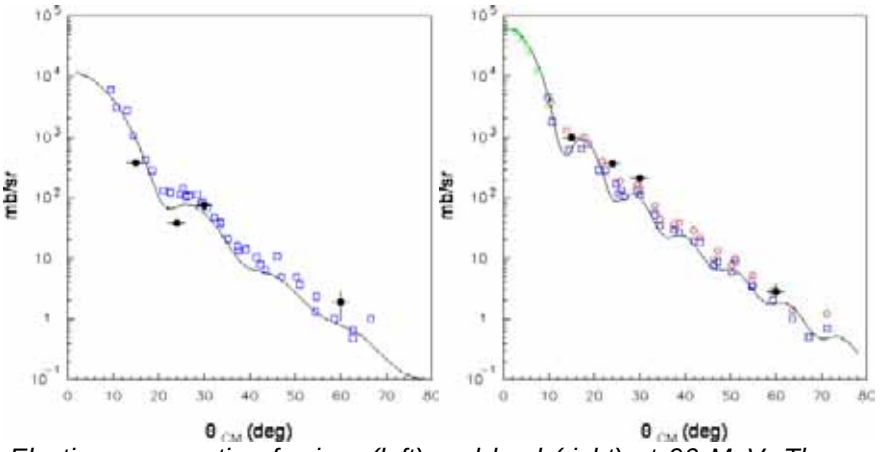

Figure 2. *Elastic cross section for iron (left) and lead (right) at 96 MeV. The experimental data are from this work (filled circles) and from previous measurements [11,12,13] (open symbols). The continuous line represents theoretical calculations based on the optical model [14].*

A detailed study shows that double differential cross section spectra at 98 degrees have all characteristics of the evaporation process in the frame of the Weisskofpt theory. The evaporation cross sections can be considered as isotropic. If we approximate elastic peak as a Gaussian function, then we can separate double differential distributions in components: evaporation, pre-equilibrium and elastic. This separation has been made for all double differential distributions presented in figure 1.

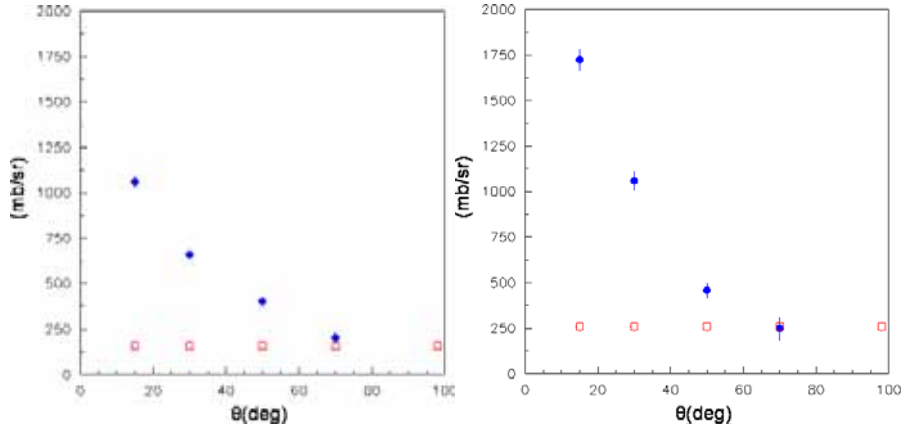

Figure 3. *Angular distributions for iron (left) and lead (right) at 96 MeV. Contribution from evaporation (open square) and pre-equilibrium (circles) process.*

Evaporation and pre-equilibrium angular distributions (figure 3) were then calculated by integration of double differential distributions. The resulting values of the pre-equilibrium emission decrease strongly with the angle preserving the same behaviour that the double differential distributions (figure 1). The data obtained for the evaporation emission are 159 ± 11 mb/sr for iron and 259 ± 23 mb/sr for lead. The relatively good agreement between these values and the values calculated using the Weisskofpt evaporation theory (respectively 148 and 306 mb/sr) suggests that double differential distributions measured at 98° are indeed the result of an evaporation process.

Energy distributions can be calculated from double differential cross sections using the Kalbach parameterization [15]. We have applied this parameterization using the complete double differential distribution (evaporation + pre-equilibrium). Results are shown in figure 4. Energy distributions have the same behaviour for iron and lead. We can observe an important

contribution at low energy due to evaporation process. This is a normal effect taking into account that neutrons are not affected by the coulomb barrier. As expected, energy cross sections for lead are higher than for iron and the difference is essentially constant over the entire energy range.

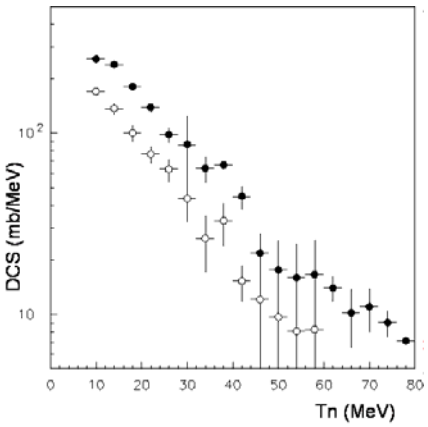

Figure 4. *Energy distributions for iron (open symbols) and lead (filled circles) derived from double differential distributions using the Kalbach parameterization [15].*

Theoretical calculations

Monte Carlo transport codes are usually employed for application, for the design and decommissioning of nuclear installations. Therefore performances of different codes and models are essential. In this section (n,Xn) energy differential distributions for lead and iron have been calculated using commonly used available transports codes and several physical models:

- MCNPX [16] with GNASH [17] and INCL4-ABLA[18,19],
- GEANT with GHEISA and FLUKA [20,21],
- TALYS [22],
- PHITS [23] with QMD [24] and SDM [25].

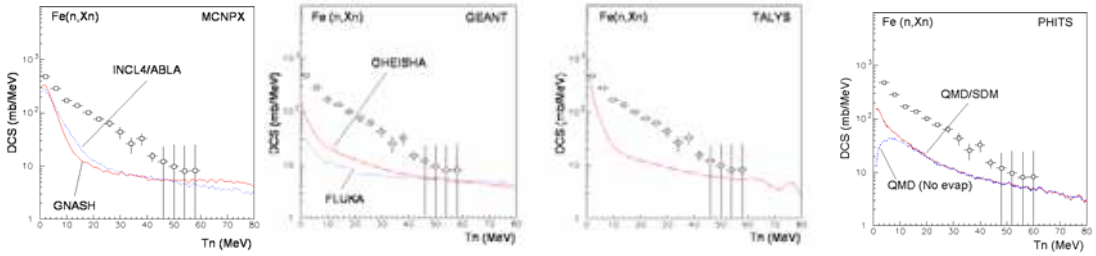

Figure 5. *Comparison between experimental data and calculated energy differential cross sections for Fe(n,Xn) reactions at 96 MeV using different available codes and models.*

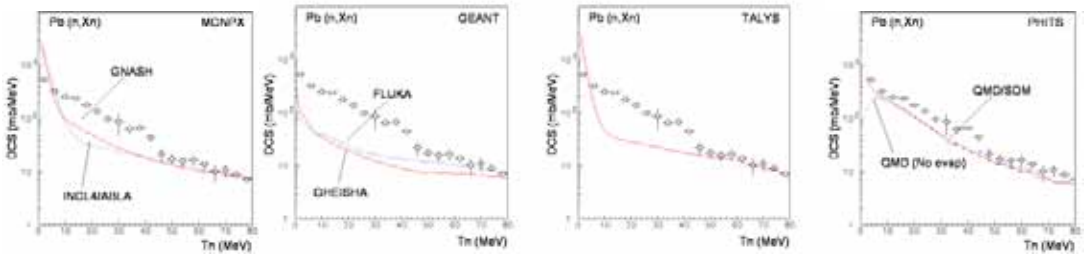

Figure 6. *Comparison between experimental data and calculated energy differential cross sections for Pb(n,Xn) reactions at 96 MeV using different available codes and models.*

Comparison between these calculations and the experimental data are shown in figures 5 and 6 for iron and lead respectively. In distribution obtained with TALYS and MCNPX we can identify two well defined contributions: an evaporative peak at low energy and a pre-equilibrium contribution at intermediate energies from 10 to 80 MeV. In distributions calculated with GEANT the effect is less visible but is also present. In these three calculated distributions, a sharp transition from pre-equilibrium to equilibrium is observed at energies around 10 MeV. Only calculations performed with QMS/SDM model using the PHITS transport show a different behaviour, allowing a better reproduction of the shape of the experimental distributions. PHITS calculation is the only one giving a reasonable agreement with measurements in all energy range in case of lead. All performed calculations give a systematic under-estimation in whole energy region in case of iron.

Cross section analysis

The EXFOR data base [26] contains few experimental data for (n,Xn) cross sections [5,27,28,29]. Available EXFOR data of double differential cross sections measured at 20° - 30° for several beam energies are presented in figure 7. One can see that the pre-equilibrium emission is not very sensitive to the incident neutron beam energy. The cross section values are comparable to the one obtains in this work.

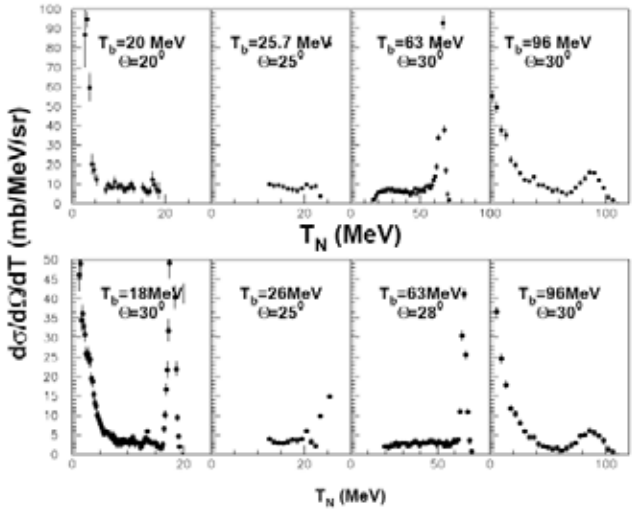

Figure 7. *Pb(n,Xn) (top) and Fe(n,Xn) (bottom) double differential cross sections at 20° - 30° for several beam energies Tb. Data are from this work and from references [5,27,28,29].*

To get a quantitative estimation of the pre-equilibrium contribution, a partial pre-equilibrium cross section σ has been derived from differential cross section by integration of the energy distribution with an energy threshold Tt. This energy threshold (Tt = 12 MeV) has been chosen to allow the use of all available data in the 18 – 100 MeV beam energy range. σ is presented as a function of the target mass (figure 8, left). Values from this work are larger than the others but we have to take into account that there is a difference of more than 70 MeV in the beam energy. To obtain a comparable quantity we have calculated the partial pre-equilibrium cross section per incident MeV. A good agreement between our data and the other experimental results is found (figure 8, right) giving confidence in data reduction and normalization procedures used in this work. Moreover a strong correlation is observed between the production ration per MeV and the size of the target.

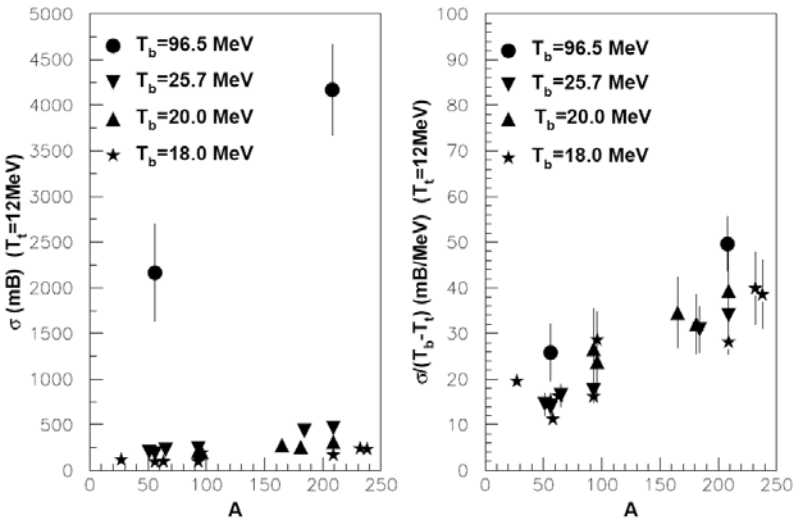

Figure 8. *Evaluated partial cross section σ with Tt = 12 MeV (left) and partial pre-equilibrium cross section per incident MeV σ / (Tb – Tt) (right) for several targets [27,28,29].*

Summary

Double differential cross sections for neutron production have been measured in 96 MeV neutrons induced reactions on iron and lead targets for an angular range between 15 and 98° and with an energy threshold of 1 – 2 MeV. Measured double differential cross section shows strong angle dependence. The elastic peak is only present at small angles (below 30°) disappearing for intermediate angles (50 – 70°) where only pre-equilibrium and evaporative contributions are present. At 98° there is only the contribution due to evaporation process.
Fe(n,n) and Pb(n,n) elastic cross sections have been extracted from double differential distributions and are in good agreement with existing experimental data and with optical model calculations. Angular distributions have been calculated for evaporative and pre-equilibrium processes. Energy distributions have been also obtained using the Kalbach systematic. Comparison between experimental data and calculations for lead show a reasonable agreement in the energy range between 40 and 80 MeV and an underestimation at low energy, except those performed with PHITS which gives a good agreement also at low energy. For iron, all calculations show a systematic underestimation in whole energy region. We have point out that only PHITS calculations are able to reproduce the shape of the measured distributions.
Comparison between the results obtained in this work and other experimental data shows that (n,Xn) double differential cross sections associated to the pre-equilibrium emission are not very sensitive to the neutron beam energy. Partial pre-equilibrium cross sections and partial pre-equilibrium cross sections per incident MeV have been calculated. Representing this as a function of target mass, a good agreement between our results and other experimental data is found.

References

[1] HINDAS. High and Intermediate energy Nuclear Data for Accelerator-Driven Systems, European Community, contract n° FI5W-CT-2000-0031.
[2] H.W. Bertini, Phys.Rev.188 (1969).
[3] A. Boudard, J. Cugnon, S. Leray and C. Volant, Phys. Rev. C66 (2002).
[4] H. Kumawat and V.S. Barashenkov, Eur. Phys. J. A26 (2005).
[5] E.L. Hjort et al, Phys. ReV. C53 (1996).
[6] EUROTRANS-NUDATRA, European Community, contract n° FI6W-CT-2004-516520.
[7] H. Condé et al, NIM A292 (1990).
[8] S. Pomp et al, ND2005, Santa Fe, AIP Conf. Proc. 769 (2005).
[9] G. Ban et al, NIM A, submitted.

[10] I.C. Sagrado Garcia et al, Proc. Intern. Workshop on Fast Neutrons Detectors and Applications, Cape Town, PoS (FNDA 2006).
[11] J. Klug et al, NIM A489 (2002).
[12] G.L. Salmon, Nucl. Phys. 21 (1960).
[13] A. Ohrn et al, to be published.
[14] A.J. Koning et J.P. Delaroche, Nucl. Phys. A713 (2003).
[15] C. Kalbach, Phys. Rev. C37 (1988).
[16] D.B. Pelowitz (Ed.), MCNPX user's Manual, LA-CP-05-0369, LANL (2005).
[17] M.B. Chadwick et al, LA-UR-98-1825, LANL (1998).
[18] A. Boudard et al, Phys. Rev. C66 (2002).
[19] A.R. Junghans et al, Nucl. Phys. A629 (1998).
[20] GEANT, CERN Program Library Long Write-up W5013.
[21] A. Fasso et al, Proc IV Int. Conf. On Calorimetry in High energy Physics, La Riodola, Italy (1993).
[22] A.J. Koning et al, NRG Report 21297/04.62741/P FAI/AK/AK (2004).
[23] H. Iwase et al, J. Nucl. Sci. Tech. 39 (2002).
[24] K. Niita et al, Phys. Rev. C52 (1995).
[25] O. Iwamoto et al, J. Nucl. Sci. Tech. 2 Suppl. (2002).
[26] EXFOR data base : http://www.nea.fr/html/dbsata/x4/.
[27] A. Marcinkowski et al, Nucl. Phys. A402 (1983) ; J. NSE 83 (1983).
[28] A. Marcinkowski et al, Nucl. Phys. A530 (1991) ; A561 (1993).
[29] S. Iijima et H. Yamakoshi, Proc. Int. Conf. Nuclear Data for Science and Technology, MITO (1988).